Mol. Cells *32*, 289-294, September 30, 2011
DOI/10.1007/s10059-011-0075-x

Molecules and Cells

Effects of Amyloid-β Peptides on Voltage-Gated L-Type $Ca_V1.2$ and $Ca_V1.3$ Ca^{2+} Channels

Sunoh Kim[1], and Hyewhon Rhim[2,*]

Overload of intracellular Ca^{2+} has been implicated in the pathogenesis of neuronal disorders, such as Alzheimer's disease. Various mechanisms produce abnormalities in intracellular Ca^{2+} homeostasis systems. L-type Ca^{2+} channels have been known to be closely involved in the mechanisms underlying the neurodegenerative properties of amyloid-β (Aβ) peptides. However, most studies of L-type Ca^{2+} channels in Aβ-related mechanisms have been limited to $Ca_V1.2$, and surprisingly little is known about the involvement of $Ca_V1.3$ in Aβ-induced neuronal toxicity. In the present study, we examined the expression patterns of $Ca_V1.3$ after $A\beta_{25-35}$ exposure for 24 h and compared them with the expression patterns of $Ca_V1.2$. The expression levels of $Ca_V1.3$ were not significantly changed by $A\beta_{25-35}$ at both the mRNA levels and the total protein level in cultured hippocampal neurons. However, surface protein levels of $Ca_V1.3$ were significantly increased by $A\beta_{25-35}$, but not by $A\beta_{35-25}$. We next found that acute treatment with $A\beta_{25-35}$ increased $Ca_V1.3$ channel activities in HEK293 cells using whole-cell patch-clamp recordings. Furthermore, using GTP pulldown and co-immunoprecipitation assays in HEK293 cell lysates, we found that amyloid precursor protein interacts with β_3 subunits of Ca^{2+} channels instead of $Ca_V1.2$ or $Ca_V1.3$ α_1 subunits. These results show that $A\beta_{25-35}$ chronically or acutely upregulates $Ca_V1.3$ in the rat hippocampal and human kidney cells (HEK293). This suggests that $Ca_V1.3$ has a potential role along with $Ca_V1.2$ in the pathogenesis of Alzheimer's disease.

INTRODUCTION

Overload of intracellular Ca^{2+} has been implicated in the pathogenesis of neuronal disorders, such as Alzheimer's disease, epilepsy, ischemia, and seizures (Choi, 1995; Kim and Rhim, 2004; Pierrot et al., 2004). In the central nervous system (CNS), mechanisms that produce abnormalities in intracellular Ca^{2+} homeostasis systems include aberrant Ca^{2+} influx through plasma membrane channels including the *N*-methyl-D-aspartic acid receptors and voltage-gated calcium channels (Cano-Abad et al., 2001; Kim et al., 2008; Luo et al., 2005; Sattler and Tymianskin, 2000). Among several types of voltage-gated Ca^{2+} channels, L-type Ca^{2+} channels have been known to be closely involved in the mechanisms underlying the neurodegenerative properties of amyloid-β (Aβ) peptides. After a report that amyloid β-protein fragment 25-35 ($A\beta_{25-35}$) causes reversible and reproducible increases in intracellular Ca^{2+} concentration ($[Ca^{2+}]_i$) along with bursts of excitatory potentials in cultured hippocampal neurons (Brorson et al., 1995), the role of L-type Ca^{2+} channels in $A\beta_{25-35}$ neurotoxicity was further examined using selective blockers of Ca^{2+} channels (Ueda et al., 1997). When L-type Ca^{2+} channels were blocked by application of nimodipine, a selective blocker for L-type Ca^{2+} channels, $A\beta_{25-35}$ neurotoxicity was attenuated. In contrast, application of ω-conotoxin GVIA or ω-agatoxin IVA, which act as blockers for N- or P/Q-type Ca^{2+} channels, had no effects on cultured rat cortical and hippocampal neurons. Later, L-type Ca^{2+} channel blockers were also found to have neuroprotective effects against Aβ-induced neuronal apoptosis in cultured rat cortical neurons (Yagami et al., 2004) and from amyloid precursor protein (APP)-induced neurotoxicity in neuroblastoma cells (Anekonda et al., 2011). Furthermore, increased intraneuronal resting $[Ca^{2+}]_i$ was reported in neurons obtained from a mouse model of Alzheimer's disease. The increased $[Ca^{2+}]_i$ was partially reduced by application of a selective L-type Ca^{2+} channel blocker, nifedipine, or a non-L-type channel blocker, SKF-96365 (Lopez et al., 2008).

Using whole-cell patch-clamp recordings, the involvement of L-type Ca^{2+} channels in Aβ-induced neuronal apoptosis has been directly demonstrated. Green and Peers (2001) have shown that Aβ selectively upregulates native L-type Ca^{2+} currents in PC12 cells, while other voltage-gated Ca^{2+} channels are unaffected. In various neuronal cells, bath application of Aβ produced a reversible increase in Ca^{2+} channel currents. This effect was blocked by treatment with nifedipine (Rovira et al., 2002; Ueda et al., 1997). In the CNS, there are 2 main types of L-type Ca^{2+} channels; $Ca_V1.2$ and $Ca_V1.3$. While the involvement of $Ca_V1.2$ in Aβ-induced neuronal apoptosis has been previously studied, the relevance of $Ca_V1.3$ to Aβ-induced neuronal apoptosis is poorly understood. Therefore, we examined the expression patterns of $Ca_V1.3$ before and after $A\beta_{25-35}$ exposure in cultured hippocampal neurons and the regulation of $Ca_V1.3$ channel currents by acute $A\beta_{25-35}$ exposure using whole-cell patch-clamp recordings in $Ca_V1.3$ expressed HEK293 cells.

[1]Jeollanamdo Institute of Natural Resources Research, Jangheung 529-851, Korea, [2]Biomedical Research Center, Korea Institute of Science and Technology, Seoul 136-791, Korea
*Correspondence: hrhim@kist.re.kr

Received April 15, 2011; revised May 18, 2011; accepted June 24, 2011; published online August 4, 2011

Keywords: Alzheimer's disease, co-immunoprecipitation, GST pulldown, intracellular Ca^{2+} L-type Ca^{2+} channels

MATERIALS AND METHODS

Materials

$A\beta_{25-35}$, $A\beta_{35-25}$, anti-β-actin, and anti-Flag antibodies were purchased from Sigma Aldrich (USA). Nifedipine was pur-chased from Tocris (USA). Anti-$Ca_V1.2$ and anti-$Ca_V1.3$ antibodies were obtained from Alomone Labs (Israel). Anti-GST and anti-myc antibodies were purchased from Novagen (USA) and Cell Signaling Technology (USA), respectively. All other chemicals were purchased from Sigma Aldrich.

RNA isolation and RT-PCR analysis

The total RNA from each sample was extracted using the easy-BLUETM kit (iNtRON Biotech, Korea) according to the manufacturer's instructions. Total RNA samples were treated with DNase I before cDNA synthesis and quantified using ultraviolet spectrophotometry. Single-strand cDNAs were then synthesized in a reverse transcription (RT) reaction in the presence of 2 μg of total RNA, 0.1 nmol of specific antisense primer, and first-strand cDNA synthesis mix (iNtRON Biotech) containing 20 mM Tris-HCl (pH 8.4), 50 mM KCl, 2.5 mM $MgCl_2$, 10 mM dithiothreitol, 0.25 mM of each dNTP, and 100 units of Moloney murine leukemia virus reverse transcriptase. The sequences of the primers and the predicted sizes of PCR products were previously reported by Kim et al. (2007). Using these primers, amplification of cDNA fragments was performed by PCR with 25-28 cycles with 1 μl of each RT product as template DNA in 60 mM Tris-HCl (pH 9.1) buffer containing 18 mM $(NH_4)_2SO_4$, 16 mM $MgCl_2$, 0.25 mM of each dNTP, 0.1 nmol of each primer, and Ex-Taq DNA polymerase (Takara, Japan). Each sample (5 μl) of final PCR product was separated using a 1.5-2.5% agarose gel and visualized using UV fluorescence after staining with ethidium bromide for 15 min. The β-actin, as a template control, was included in each run.

Cell culture and transfection

HEK293 cells were grown in Dulbecco's modified Eagle's medium supplemented with 10% fetal bovine serum, penicillin (100 units/ml), and streptomycin (100 μg/ml) in a humidified atmosphere of 5% CO_2 and 95% air at 37°C. For electrophysiological recordings of $Ca_V1.3$ channel currents, HEK293 cells were transiently transfected with $Ca_V1.3$ α_1 and β_3 subunits using Lipofectamine 2000 (Invitrogen, USA). Cultured hippocampal neurons were prepared using a technique modified from Kim et al. (2007). Briefly, the hippocampi were isolated from 18-day-old fetal Sprague-Dawley rats and incubated with 0.25% trypsin in Leibovitz L-15 medium (Invitrogen). Cells were then mechanically dissociated and plated on poly-L-lysine-coated culture dishes. Cultures were maintained in Neurobasal/B27 medium (Invitrogen) containing 0.5 mM L-glutamine, 25 μM 2-mercaptoethanol, 100 units/ml penicillin, and 100 μg/ml streptomycin under a humidified atmosphere of 95% air and 5% CO_2 at 37°C. Experiments were carried out on neurons after 5-10 days *in vitro*.

Western blot analysis of $Ca_V1.2$ or $Ca_V1.3$ protein expression

For the detection of $Ca_V1.2$ or $Ca_V1.3$, cultured hippocampal neurons were treated with $A\beta_{25-35}$ or $A\beta_{35-25}$ for 24 h, and the prepared protein samples were separated on 6% SDS-PAGE. The proteins then transferred to a polvinylidene difluoride membrane (Millipore, USA). The membrane was first blocked with PBS containing 5% skim milk and 0.1% Tween 20 for 1 h. After 3 washes, the membranes were incubated with anti-$Ca_V1.2$ (1:150 dilution) or anti-$Ca_V1.3$ (1:150 dilution) antibodies for 20 h at room temperature in PBS containing 1% skim milk and 0.1% Tween 20. For a positive control, anti-β-actin antibodies (1:2500 dilution) were incubated for 1 h. After 3 washes, the membranes were incubated with peroxidase-conjugated secondary antibodies in PBS containing 3% skim milk and 0.1% Tween 20 for 2 h at room temperature. The signal resulting from the immunoreactivity was detected using a western blot detection reagent (Elipis Biotech, Korea). For the detection of each channel's surface protein, biotinylation of cell surface proteins was performed using the Pinpoint Cell Surface Protein Isolation kit (Pierce) according to the manufacturer's instructions as previously described by Yun et al. (2007).

Electrophysiological recording

$Ca_V1.3$ channel currents were measured in HEK293 cells transfected with $Ca_V1.3$ α_1 subunits using Ba^{2+} as a charge carrier with standard whole-cell patch-clamp techniques. Borosilicate glass electrodes were filled with the internal solution containing (in mM): 135 CsCl, 10 EGTA, 4 $MgCl_2$, 10 HEPES, and 4 Mg-ATP (pH 7.4). The external solution contained (in mM): 135 CholineCl, 5 $BaCl_2$, 1 $MgCl_2$, 10 glucose, and 10 HEPES (pH 7.4). Cells were held at a holding potential of -70 mV, and currents were elicited with step depolarizations from -60 mV to +30 mV (10 mV increments) for 200 ms. All of the data were obtained and analyzed using an EPC-10 amplifier and Pulse/Pulsefit software program (HEKA, Germany).

GST pulldown assays

GST pulldown assays were performed with purified GST and various GST-tagged proteins using the ProFound Pull-Down GST Protein:Protein Interaction Kit (Pierce, USA). The immobilized GST or various GST-tagged proteins were incubated with cell lysates prepared from HEK293 cells. Glutathione-bound proteins were eluted by boiling at 95°C in SDS sample buffer for 10 min, and detected by immunoblotting with anti-$Ca_V1.2$, anti-$Ca_V1.3$, anti-GST, or anti-Flag antibodies.

Co-immunoprecipitation assay

Co-immunoprecipitation (co-IP) assays were performed using the ProFound Mammalian Co-Immunoprecipitation Kit (Pierce). Briefly, lysates from HEK293 cells were precleared, immunoprecipitated with 10 μg of a specific antibody and 50 μl of AminoLink® Plus Coupling Gel at 4°C for 6 h or overnight, and washed 5 times. Immune complexes were eluted using IgG Elution Buffer (Pierce) or by boiling at 95°C in SDS-sample buffer for 10 min, and detected by immunoblotting with anti-$Ca_V1.2$, anti-$Ca_V1.3$, anti-myc, or anti-Flag antibodies.

RESULTS AND DISCUSSION

To elucidate the involvement of $Ca_V1.3$ L-type Ca^{2+} channels in the mechanisms underlying the neurodegenerative properties of Aβ peptides, we examined the expression profiles of $Ca_V1.2$ and $Ca_V1.3$ before and after treatment with $A\beta_{25-35}$ in cultured rat hippocampal neurons. Treatment with 25 nM $A\beta_{25-35}$ for 24 h significantly increased both total and surface $Ca_V1.2$ protein levels as well as $Ca_V1.2$ mRNA levels while there was no significant change observed upon treatment with the inverted sequence of $A\beta_{25-35}$, amyloid β-protein fragment 35-25 ($A\beta_{35-25}$) (Figs. 1A-1C). However, the expression levels of $Ca_V1.3$ were not significantly changed by either $A\beta_{25-35}$ or $A\beta_{35-25}$ both at the mRNA and total protein levels. Interestingly, $Ca_V1.3$ proteins were significantly increased only at the surface level by $A\beta_{25-35}$, but not by$A\beta_{35-25}$ (Fig. 1C). For $Ca_V1.2$, we also observed the increased surface level by $A\beta_{25-35}$, but not by$A\beta_{35-25}$. Figure 1D displays the summarized data showing the effects of $A\beta_{25-35}$ or

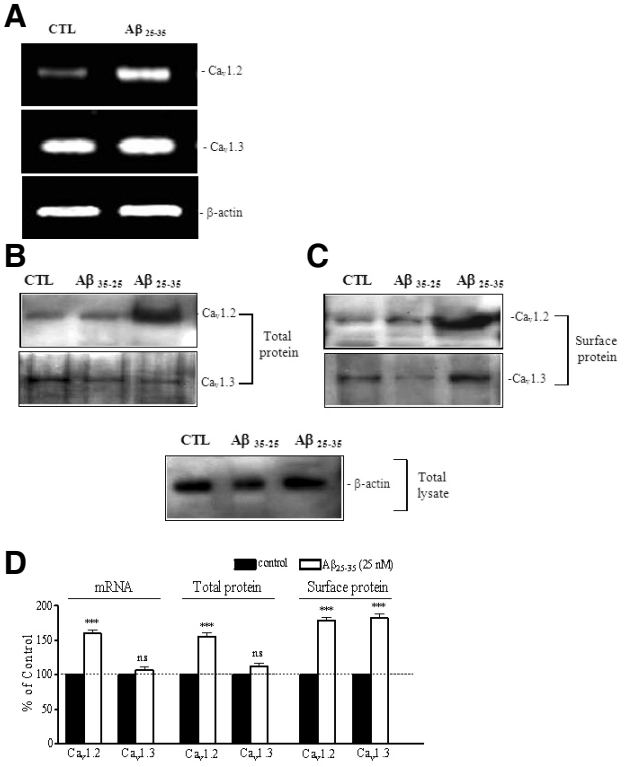

Fig. 1. Effects of Aβ exposure on expression profiles of $Ca_V1.2$ and $Ca_V1.3$ in hippocampal neurons. (A) Expression levels of $Ca_V1.2$ and $Ca_V1.3$ mRNAs in the presence of $A\beta_{25\text{-}35}$ (25 nM) for 24 h. $Ca_V1.2$ and $Ca_V1.3$ mRNAs were determined using RT-PCR analysis from cell lysates obtained from cultured hippocampal neurons. (B and C) Expression levels of total (B) or surface (C) $Ca_V1.2$ and $Ca_V1.3$ proteins in the presence of $A\beta_{35\text{-}25}$ or $A\beta_{25\text{-}35}$. $Ca_V1.2$ (240 kDa) and $Ca_V1.3$ (260 kDa) proteins were determined using western blot analysis with anti-$Ca_V1.2$ and anti-$Ca_V1.3$ antibodies, respectively. β-Actin was used as a positive control for RT-PCR and Western blot analyses. (D) The bar graph indicates the mean values of relative mRNA or protein levels from each group ($n = 3$). The level of control mRNA or protein was counted as an arbitrary control (100%). ***, $p < 0.001$ compared with the control level.

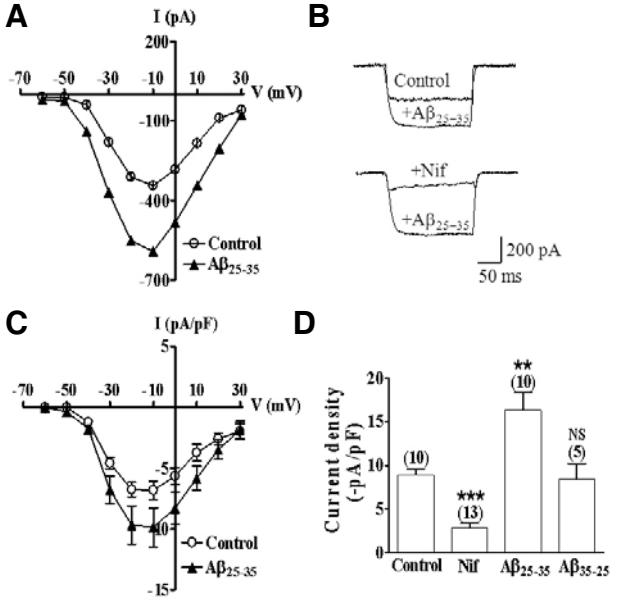

Fig. 2. Effects of Aβ acute exposure on Ca^{2+} channel currents in HEK 293 cells stably expressing the human $Ca_V1.3$ α_1 subunit. (A) Current-voltage (*I-V*) relationships of peak $Ca_V1.3$ currents in the absence (open circles) or presence (filled triangles) of 25 nM $A\beta_{25\text{-}35}$. (B) Upper traces: representative example currents showing $A\beta_{25\text{-}35}$-induced upregulation of $Ca_V1.3$ currents. Lower traces: example currents showing the effects of bath application of nifedipine (Nif, 10 μM). Ca^{2+} channel currents were evoked by a step depolarization applied from -70 mV to -10 mV for 200 ms. (C) Mean current density-voltage relationships obtained from control cells (open circles) and from cells acutely exposed to 25 nM $A\beta_{25\text{-}35}$ during whole-cell patch-clamp recordings (filled triangles). (D) Pooled results illustrating the mean current density of peak $Ca_V1.3$ channel currents in the presence of nifedipine, $A\beta_{25\text{-}35}$ or $A\beta_{35\text{-}25}$. ***, $p < 0.001$; **, $p < 0.01$ compared with the control level. NS, not significant.

$A\beta_{35\text{-}25}$ on relative mRNA or protein levels of $Ca_V1.2$ and $Ca_V1.3$. These results suggest that $A\beta_{25\text{-}35}$-induced expression profiles of $Ca_V1.3$ mRNA and total proteins are different from the profiles of $Ca_V1.2$, and both channels are similarly upregulated at the surface level only in an $A\beta_{25\text{-}35}$ specific manner in cultured hippocampal neurons.

We next examined whether acute treatment with $A\beta_{25\text{-}35}$ modulates $Ca_V1.3$ channel activities using whole-cell patch-clamp recordings. When $Ca_V1.3$ α_1 and β_3 subunits were transiently transfected in HEK293 cells, GFP was also co-transfected to identify positively transfected cells. Using Ba^{2+} as a charge carrier, $Ca_V1.3$ channel currents were measured in transfected cells only as previously described in Park et al. (2010). When $A\beta_{25\text{-}35}$ was applied to the perfusate, Ba^{2+} currents were rapidly increased. This was maximally observed at a test pulse of -10 mV (Fig. 2A). In Fig. 2B, upper representative traces of the $Ca_V1.3$ recordings show an increase in Ba^{2+} currents upon addition of 25 nM $A\beta_{25\text{-}35}$. Lower traces show a decrease in Ba^{2+} currents upon addition of 10 μM nifedipine, a selective L-type Ca^{2+} channel blocker. These results suggest that Ba^{2+} currents were predominantly recorded via an activation of $Ca_V1.3$ channels. $A\beta_{25\text{-}35}$ significantly increased the peak currents of $Ca_V1.3$ (8.93 ± 0.65 pA/pF in control; 16.40 ± 1.97 pA/pF in the presence of $A\beta_{25\text{-}35}$, $n = 10$), but did not cause any shift in the current-voltage curve in Fig. 2C. Addition of $A\beta_{35\text{-}25}$ at the same concentration as $A\beta_{25\text{-}35}$ (25 nM) did not produce any effect on peak currents of $Ca_V1.3$ ($n = 5$). This is summarized in Fig. 2D. These results provide the first experimental evidence that acute treatment with $A\beta_{25\text{-}35}$ increases $Ca_V1.3$ L-type Ca^{2+} currents in HEK293 cells.

For the possible mechanisms of Aβ-induced upregulation of $Ca_V1.3$, we attempted to determine whether a direction association occurs between α_1 subunits of L-type Ca^{2+} channels and full length amyloid precursor protein (APP695). We performed GST pulldown assays using GST-tagged APP695 and a GST-tagged fragment of APP695, which contains the amino acid sequence from 306 to 695 (APP390, Fig. 3A). After GST, GST-APP695, and GST-APP390 were expressed in *Escherichia coli*, they were immobilized by glutathione-agarose 4B. Then, the lysates from the HEK293 cells overexpressing α_1 subunits of $Ca_V1.2$ or $Ca_V1.3$ were incubated with the glutathione-agarose 4B bound to GST-APP695 or GST-APP390. As shown in Fig. 3B and 3C, GST-APP695 was shown not to interact with either $Ca_V1.2$ or $Ca_V1.3$. Using GST-APP390, we also found that there is no interaction of $Ca_V1.2$ or $Ca_V1.3$ with APP390. There-

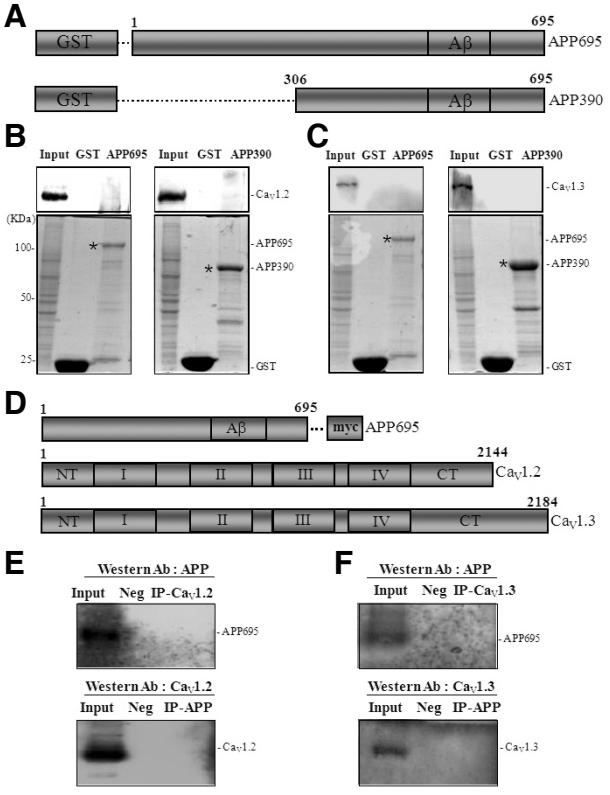

Fig. 3. The GST pulldown assay between APP and $Ca_V1.2$ or $Ca_V1.3$. (A) Schematic diagram of GST-tagged full-length amyloid precursor protein (APP695) and a fragment of APP695, which contains the amino acid sequence from 306 to 695 (APP390). (B) Immobilized GST, GST-APP695, or GST-APP390 was incubated with cell lysate, and then the retained proteins were analyzed with anti-$Ca_V1.2$ or anti-GST antibodies. (C) Immobilized GST, GST-APP695, or GST-APP390 was incubated with cell lysate, and then the retained proteins were analyzed with anti-$Ca_V1.3$ or anti-GST antibodies. (D) Schematic diagram of myc-tagged APP695, $Ca_V1.2$ and $Ca_V1.3$. (E, F) *In vivo* co-IP assays. Where specified, the solubilized total proteins (100 μg) from HEK293 cells were immunoprecipitated with anti-$Ca_V1.3$, anti-$Ca_V1.2$, or anti-APP antibo-dies. The immune complexes were then analyzed by SDS-PAGE, followed by immunoblotting with anti-APP antibodies (E, F), anti-$Ca_V1.2$ (E) or anti-$Ca_V1.3$ (F) antibodies.

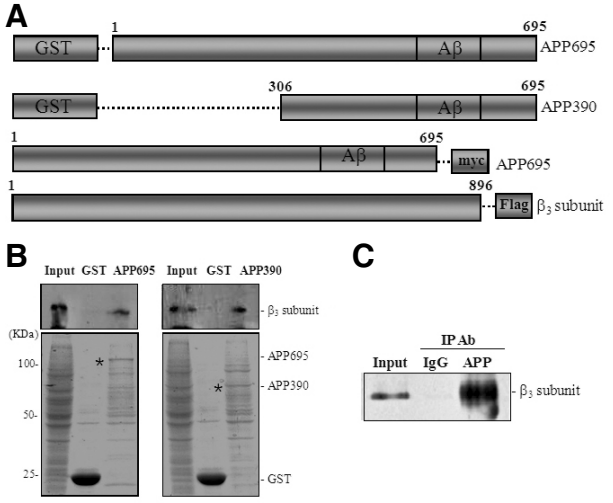

Fig. 4. Interaction between APP and β_3 subunit using GST pull-down and co-IP assays. (A) Schematic diagram of GST-tagged APP695, GST-tagged APP390, myc-tagged APP695, and Flag-tagged β_3 subunit. (B) Immobilized GST, GST-APP695, or GST-APP390 was incubated with cell lysate, and then the retained proteins were analyzed with anti-β_3 subunit or anti-GST antibodies. (C) Solubilized total proteins (100 μg) from HEK293 cells were immunoprecipitated with anti-APP antibodies, and the immune complexes were detected with anti-β_3 antibodies.

fore, using an *in vivo* co-IP assay, we further examined a direct interaction between L-type Ca^{2+} channels and APP695 in HEK293 cells overexpressing myc-tagged APP695 and one of the L-type Ca^{2+} channels (Fig. 3D). For the $Ca_V1.2$ channels, cell lysates were prepared, immunoprecipitated with anti-$Ca_V1.2$ antibodies, and subsequently immunoblotted with anti-myc antibodies. As shown in Fig. 3E, no positive signal was detected. When co-IP was performed in reverse with anti-myc antibodies followed by immunoblotting with anti-$Ca_V1.2$, the result was the same. For the examination of a direct interaction between $Ca_V1.3$ with APP695, cell lysates were prepared, immunoprecipitated with anti-$Ca_V1.3$ antibodies, and subsequentlly immunoblotted with anti-myc antibodies. In addition, co-IP was performed in reverse with anti-myc antibodies followed by immunoblotting with anti-$Ca_V1.3$. However, we found that there is no association between $Ca_V1.3$ and APP695 in HEK293 cells (Fig. 3F).

Then, what is the mechanism of Aβ-induced upregulation of $Ca_V1.3$ evidenced by the data shown in Figs. 1 and 2? In native brain tissues, α_1 subunits of Ca^{2+} channels interact with other auxiliary subunits, e.g., $\alpha_2\delta$, β, and γ subunits, to provide complete activity and functional regulation. In a heterologous expression system such as the HEK293 cells used in this study, other auxiliary subunits of Ca^{2+} channels are required when α_1 subunits are expressed for their full activation. In the present study, we used HEK293 cells transfected with $Ca_V1.3$ α_1 and β_3 subunits. Therefore, we examined the possible involvement of β_3 subunits as modulators of Aβ-induced upregulation of L-type Ca^{2+} channels. We performed GST pulldown assays to observe the specific interaction between APP and β_3 subunits. As shown in Figs. 4A and 4B, GST-APP695 or GST-APP390 interacts with Flag-tagged β_3 subunits in HEK293 cell lysates expressing β_3 subunits while GST alone (a negative control) was found to not interact with the β_3 subunits. Subsequently, using an *in vivo* co-IP assay, we confirmed the association of APP and β_3 subunits in HEK293 cells expressing myc-tagged APP695 and Flag-tagged β_3 subunits. Cell lysates prepared from HEK293 cells were immunoprecipitated with anti-myc antibodies, and subsequently immunoblotted with anti-Flag antibodies. In Fig. 4C, APP binds to endogenous β_3 subunits in HEK293 cells whereas no signal was detected in an IgG control. These results strongly suggest that a specific interaction between APP and β_3 subunits occurs in mammalian cells.

Herein, we present 3 principal findings regarding possible roles of $Ca_V1.3$ in Aβ-induced neuronal toxicity. First, we found that the expression levels of $Ca_V1.3$ are moderated only at the surface protein level by chronic treatment with Aβ. This pattern is the different from the $Ca_V1.2$ pattern. In the current study, the 24 h treatment with $A\beta_{25\text{-}35}$ significantly increased both total and surface $Ca_V1.2$ protein levels as well as $Ca_V1.2$ mRNA levels while there was no significant change when $A\beta_{35\text{-}25}$, the reverse amino acid sequence peptide of $A\beta_{25\text{-}35}$, was used. In addition,

Aβ-mediated upregulation of $Ca_V1.2$ was previously reported with respect to mRNA and total protein levels (Chiou, 2006) as well as surface protein levels (Scragg et al., 2004). Our results with respect to $Ca_V1.3$ mRNA and total protein levels were consistent with the previous findings using human SK-N-SH neuroblastoma cells. When the expression patterns of 4 α_1 subunits of P/Q ($Ca_V2.1$)-, N ($Ca_V2.2$)-, and L ($Ca_V1.2$ and $Ca_V1.3$)-type Ca^{2+} channels before and after Aβ exposure were investigated in SK-N-SH cells, no significant changes were observed with respect to $Ca_V1.3$ mRNA and total protein levels (Chiou, 2006). Because the surface protein levels were not examined by Chiou (2006), we first reported that the 24 h treatment with Aβ selectively upregulates the $Ca_V1.3$ surface expression in cultured hippocampal neurons.

Secondly, we found that acute treatment with $A\beta_{25-35}$ increased $Ca_V1.3$ channel activities using whole-cell patch-clamp recordings in HEK293 cells. Direct evidence for the involvement of L-type Ca^{2+} channels in Aβ-induced neuronal toxicity was obtained from the electrophysiological studies of endogenous L-type Ca^{2+} channels in neurons or cell lines expressing $Ca_V1.2$ in heterologous systems (Green and Peers, 2001; Rovira et al., 2002; Ueda et al., 1997). Because there were no reports examining the acute effects of Aβ on $Ca_V1.3$ channel activities using electrophysiological tools, we attempted to examine them in HEK293 cells transiently expressing $Ca_V1.3$ α_1 and β_3 subunits. On the basis of our data, it appears that $Ca_V1.3$ could be directly modulated by Aβ, and the degree of upregulation is very similar to that of $Ca_V1.2$ determined in HEK293 cells (Scragg et al., 2004). Although the augmentation of currents by $A\beta_{25-35}$ is apparent in the present study, it is also interesting to examine effects of the predominant 2 toxic forms of Aβ peptides, $A\beta_{1-40}$ and $A\beta_{1-42}$, on $Ca_V1.3$ channel activities.

What is a possible mechanism of Aβ-induced upregulation of $Ca_V1.2$ and $Ca_V1.3$ both chronically and acutely? As the third and final piece of evidence on the possible roles of $Ca_V1.3$ in Aβ-induced neuronal toxicity, we found that β_3 auxiliary subunits of Ca^{2+} channels may play an important role in Aβ-induced upregulation of $Ca_V1.2$ and $Ca_V1.3$. On the basis of experiments using GST pulldown and co-IP assays, we clearly determined that neither $Ca_V1.2$ nor $Ca_V1.3$ binds to APP in both the GST pulldown and the co-IP experiments. However, we demonstrated that β_3 subunits of Ca^{2+} channels interact with APP695 or APP390. This suggests a possible role of β_3 subunits of Ca^{2+} channels in Aβ-induced neuronal toxicity. It is possible that APP, which contains the Aβ fragment, increases surface expression of $Ca_V1.3$ or functional activities of $Ca_V1.3$ via an interaction with β_3 subunits. However, for the detailed mechanism of Aβ-induced upregulation of $Ca_V1.3$, it is necessary to demonstrate whether Aβ interacts with β_3 subunits in the brain using binding assays or to elucidate binding sequences of APP using mapping studies.

A number of recent studies have shown that Aβ can disrupt neuronal Ca^{2+} homeostasis by inducing influx of extracellular Ca^{2+} into the neuronal cytoplasm (Anekonda et al., 2011; Small et al., 2009; Supnet and Bezprozvanny, 2010). Among the functions of voltage-gated Ca^{2+} channels regulating neuronal excitability, synaptic plasticity, and neurotoxicity, functions of the neuronal L-type Ca^{2+} channels are distinguished from the functions of the N- and P/Q-type Ca^{2+} channels. N- and P/Q-type Ca^{2+} channels clearly play central roles in controlling Ca^{2+} entry into, and thus neurotransmitter release from, neuronal synaptic terminals in the CNS (Catterall, 1999; Dunlap et al., 1995). On the other hand, neuronal L-type Ca^{2+} channels are known to be involved in translating synaptic activity into alterations in gene expression and neuronal cell death (Cano-Abad et al., 2001; Finkbeiner and Greenberg, 1997; Fuchs, 1996; Luo et al., 2005). This is related to the Aβ specific increases in the quantity and activity of L-type Ca^{2+} channels caused by Aβ. Among the possible mechanisms underlying Aβ-induced Ca^{2+} dysregulation, Aβ can increase ion permeability in lipid membranes or activate endogenous ion channels on the cell surface (Small et al., 2009). In the present study, we showed that Aβ does not change the amount of mRNA of $Ca_V1.3$ but dramatically alters the quantity of surface proteins of $Ca_V1.3$. This provides further support for the results showing that Aβ activates endogenous ion channels on the cell surface. Therefore, the Aβ-induced increase in surface proteins of $Ca_V1.3$ could provide more surface-expressed L-type Ca^{2+} channels, which deteriorate and cause neuronal cell death *via* Ca^{2+} overload.

In summary, using expression profiling and electrophysiological studies as well as *in vivo* binding assays, we showed the first evidence of Aβ-mediated upregulation of $Ca_V1.3$ surface proteins and $Ca_V1.3$ channel activities and further originally demonstrated direct binding between APP and β_3 subunits of Ca^{2+} channels. These results may help elucidate pivotal roles of L-type Ca^{2+} channels in intracellular Ca^{2+} disturbance in Alzheimer's disease. It is likely that elucidation of the mechanism by which Aβ cause Ca^{2+} dysregulation via L-type Ca^{2+} channels will help identify new drug targets for the treatment of Alzheimer's disease.

ACKNOWLEDGMENTS

This work was supported by a Mid-Career Researcher Program Grant (No. 20110000094), a Pioneer Grant (No. 20110002117), and the BRC of the 21st Century Frontier Research Program (No. 2011K000272) to H. Rhim and a Basic Science Research Program (2009-0076837) to S. Kim from the Ministry of Education, Science and Technology, the Republic of Korea.

REFERENCES

Anekonda, T.S., Quinn, J.F., Harris, C., Frahler, K., Wadsworth, T. L., and Woltjer, R.L. (2011). L-type voltage-gated calcium channel blockade with isradipine as a therapeutic strategy for Alzheimer's disease. Neurobiol. Dis. *41*, 62-70.

Brorson, J.R., Bindokas, V.P., Iwama, T., Marcuccilli, C.J., Chisholm, J.C., and Miller, R.J. (1995). The Ca^{2+} influx induced by beta-amyloid peptide 25-35 in cultured hippocampal neurons results from network excitation. J. Neurobiol. *26*, 325-338.

Cano-Abad, M.F., Villarroya, M., Garcia, A.G., Gabilan, N.H., and Lopez, M.G. (2001). Ca^{2+} entry through L-type Ca^{2+} channels causes mitochondrial disruption and chromaffin cell death. J. Biol. Chem. *276*, 39695-39704.

Catterall, W.A. (1999). Interactions of presynaptic Ca^{2+} channels and snare proteins in neurotransmitter release. Ann. N. Y. Acad. Sci. *868*, 144-159.

Chiou, W.F. (2006). Effect of Abeta exposure on the mRNA expression patterns of voltage-sensitive calcium channel alpha 1 subunits (alpha 1A-alpha 1D) in human SK-N-SH neuroblastoma. Neurochem. Int. *49*, 256-261.

Choi, D.W. (1995). Ca^{2+}: still center-stage in hypoxic-ischemic neuronal death. Trends Neurosci. *18*, 58-60.

Dunlap, K., Luebke, J.I., and Turner, T.J. (1995). Exocytotic Ca^{2+} channels in mammalian central neurons. Trends Neurosci. *18*, 89-98

Finkbeiner, S., and Greenberg, M.E. (1997). Spatial features of calcium-regulated gene expression. BioEssays *19*, 657-660.

Fuchs, P.A. (1996). Synaptic transmission at vertebrate hair cells. Curr. Opin. Neurobiol. *6*, 514-519.

Green, K.N., and Peers, C. (2001). Amyloid beta peptides mediate hypoxic augmentation of Ca(2+) channels. J. Neurochem. *77*, 953-956.

Kim, S., and Rhim, H. (2004). Ginsenosides inhibit NMDA receptor-mediated epileptic discharges in cultured hippocampal neurons. Arch. Pharm. Res. *27*, 524-530.

Kim, S., Yun, H.M., Baik, J.H., Chung, K.C., Nah, S.Y., and Rhim, H. (2007). Functional interaction of neuronal Cav1.3 L-type calcium channel with ryanodine receptor type 2 in the rat hippocampus. J. Biol. Chem. *282*, 32877-32889.

Kim, S., Nah, S.Y., and Rhim, H. (2008). Neuroprotective effects of ginseng saponins against L-type Ca^{2+} channel-mediated cell death in rat cortical neurons. Biochem. Biophys. Res. Commun. *365*, 399-405.

Lopez, J.R., Lyckman, A., Oddo, S., Laferla, F.M., Querfurth, H.W., and Shtifman, A.J. (2008). Increased intraneuronal resting [Ca^{2+}] in adult Alzheimer's disease mice. J. Neurochem. *105*, 262-271.

Luo, C.X., Zhu, X.J., Zhang, A.X., Wang, W., Yang, X.M., Liu, S.H., Han, X., Sun, J., Zhang, S.G., Lu, Y., et al. (2005). Blockade of L-type voltage-gated Ca^{2+} channel inhibits ischemia-induced neurogenesis by down-regulating iNOS expression in adult mouse. J. Neurochem. *94*, 1077-1086.

Park, H.W., Jung, H., Choi, K.H., Baik, J.H., and Rhim, H. (2010). Direct interaction and functional coupling between voltage-gated $Ca_V1.3$ Ca^{2+} channel and $GABA_B$ receptor subunit 2. FEBS Lett. *584*, 3317-3322.

Pierrot, N., Ghisdal, P., Caumont, A.S., and Octave, J.N. (2004). Intraneuronal amyloid-beta1-42 production triggered by sustained increase of cytosolic calcium concentration induces neuronal death. J. Neurochem. *88*, 1140-1150.

Rovira, C., Arbez, N., and Mariani, J. (2002). Abeta (25-35) and Abeta (1-40) act on different calcium channels in CA1 hippocampal neurons. Biochem. Biophys. Res. Commun. *296*, 1317-1321.

Sattler, R., and Tymianski, M. (2000). Molecular mechanisms of calcium dependent excitotoxicity. J. Mol. Med. *78*, 3-13.

Scragg, J.L., Fearon, I.M., Boyle, J.P., Ball, S.G., Varadi, G., and Peers, C. (2004). Alzheimer's amyloid peptides mediate hypoxic up-regulation of L-type Ca^{2+} channels. FASEB J. *19*, 150-152.

Small, D.H., Gasperini, R., Vincent, A.J., Hung, A.C., and Foa, L. (2009). The role of Abeta-induced calcium dysregulation in the pathogenesis of Alzheimer's disease. J. Alzheimers Dis. *16*, 225-233.

Supnet, C., and Bezprozvanny, I. (2010). The dysregulation of intracellular calcium in Alzheimer disease. Cell Calcium *47*, 183-189.

Ueda, K., Shinohara, S., Yagami, T., Asakura, K., and Kawasaki, K. (1997). Amyloid beta protein potentiates Ca^{2+} influx through L-type voltage-sensitive Ca^{2+} channels: a possible involvement of free radicals. J. Neurochem. *68*, 265-271.

Yagami, T., Ueda, K., Sakaeda, T., Itoh, N., Sakaguchi, G., Okamura, N., Hori, Y., and Fujimoto, M. (2004). Protective effects of a selective L-type voltage-sensitive calcium channel blocker, S-312-d, on neuronal cell death. Biochem. Pharmacol. *67*, 1153-1165.

Yun, H.M., Kim, S., Kim, H.J., Kostenis, E., Kim, J.I., Seong, J.Y., Baik, J.H., and Rhim, H. (2007). The novel cellular mechanism of human 5-HT6 receptor through an interaction with Fyn. J. Biol. Chem. *282*, 5496-5505.